Corrosion Performance of Multiple Principal Elements containing Alloys

Balwinder Singh[a], Sangamdeep Singh[b], Saurabh Sharma[b]

[a]M.Tech Scholar, Department of Mechanical Engineering, Sri Sai College of Engineering & Technology, Badhani

[b]Assistant Professor,Department of Mechanical Engineering Sri Sai College of Engineering & Technology, Badhani

---

Abstract: The multiple principal elements containing HEAs generally contain 5-13 elements with atomic percentage in between 5 and 35 for each element. The minimum 5 elements are taken to get enough entropy to avoid the intermetallic formation and segregation of elements. The maximum 13 elements are taken because beyond this limit, there is not significant contribution to entropy however the complexity increases. In addition to the multiple elements, some minor elements can also be added with atomic % below 5%. The current research concerns with the characterization and corrosion performance of high entropy alloys. For the preparation of HEAs, melting and casting route was adopted by converting the green compacted pellets in to button shaped final samples. All the samples were characterized using X-ray diffraction (XRD) and optical microscopy. Also, the hardness of the samples was assessed. The corrosion behavior of the samples was investigated using the potentiostat in 3.5.% NaCl solution.

Keywords: *High-entropy alloys, Electrochemical Corrosion, Corrosion current density, Corrosion potential*

1. INTRODUCTION: The practice of alloying has been steadily improving since the Bronze Age, with significant improvements along the way. It has lately been a popular study topic to focus on improving revolutionary multi-element alloys in order to fulfill the needs of sophisticated applications that require greater performance. Traditional alloys are primarily comprised of one or two basic elements that have been selected to meet a particular property need for a certain use, with further alloying additions improving those capabilities. High-entropy alloys (HEAs), on the other hand, are a relatively recent idea in alloy design that comprises five or more main elements, each of which is mixed individually before being combined together. The investigation of HEAs began in 2004 with the completion of two separate investigations. Cantor et al. [2] and Yeh et al. [3] both took the initiative to deal with alloys in the center of the phase diagram rather than towards the apexes or edges of the phase diagram, respectively. In a successful synthesis of an equi-atomic FeCrMnCoNi alloy with a single FCC phase, Cantor et al. [2] demonstrated the presence of dendritic (having almost equal proportions of each element) and inter-dendritic (low in Fe but rich in Cr and Mn) regions in the microstructure, as well as the presence of dendritic (having almost equal proportions of each element) regions. When the sixth element (Nb, Ti, V, Cu, Ge, one by one) was introduced into this alloy, it was discovered that the FCC phase of FeCrMnCoNi was capable of dissolving significant amounts of Nb, Ti, and V but not significant amounts of Cr and Ge due to the higher electronegativity of the latter two elements. For the first time, Yeh and his colleagues [3] published well-explained research on multi-component alloys that was favorably received. Yeh designated these alloys as 'High Entropy Alloys (HEAs)' because he believed that the entropy of mixing for equimolar alloys containing more than five major elements would be adequate to reduce the propensity of ordering and segregation, as a result of which simple phases would occur. In his definition, high entropy alloys are equi-molar alloys containing five or more primary components in equal proportions. Adding boron (B) to CuCoNiCrAl0.5Fe HEA (Yeh's HEA) resulted in a single FCC phase, as validated by XRD analysis, which confirmed a single FCC phase for all CuCoNiCrAl0.5FeBx HEAs, in which peak intensities of Cr and Fe borides emerged and rose by increasing the quantity of B, respectively.

A number of Mn-containing high-strength and/or high-ductility HEAs have been described [4, 5, 6, and 7], although the majority of them would have limited anticorrosive performance due to their Mn content. Several investigations on the creation of innovative HEAs [8-13] have shown that striking a balance between corrosion resistance and mechanical qualities has been difficult to accomplish in earlier studies on this topic. The alloy AlxCoCrFeNi (x = 0.3, 0.5, and 0.7) had high corrosion resistance in 3.5 weight percent NaCl [13], but it exhibited low ductility owing to the brittle BCC eutectic phase in the alloy [14]. Similarly, in the case of Mo-doped FeNiCoCr alloys [24], a similar situation has been described. Furthermore, it has been shown that the alloying of Cu in the FeCoNiCrCux system (x = 0, 0.5, and 1) not only accelerates localized corrosion but also degrades plasticity due to the creation of a Cu-rich inter-dendritic phase [12]. In fact, for structural materials that are used in

severe environments, a good mix of mechanical characteristics and anti-corrosion performance is required [14]. Consequently, it is critical to investigate corrosion-resistant alloys that have outstanding mechanical properties.

2. MATERIALS AND METHODS

Al, Co, Cr, Cu, Fe, Ni, and Ti powders were used as raw materials for the present work. Table 1 shows the composition of HEAs investigated in the present study.

Table 1 Composition of high entropy alloy system

Alloy	Al	Co	Cr	Cu	Fe	Ni	Ti
HEA1	4	18	18	2	18	35	5
HEA2	4	18	18	2	18	33	7
HEA3	4	18	18	2	18	31	9
HEA4	4	18	18	2	18	30	10

The powders as per the compositions were blended and converted into cylindrical pellet using 15 mm die by applying 120 MPa pressure. The HEAs were made in an inert environment using the arc melting procedure. The alloys were then analysed, and the HEAs' corrosion behaviour in NaCl solution was examined. The melting and flipping of the samples were performed 5 times for homogeneous structure.

3. CHARACTERIZATION OF SAMPLES

3.1 X-Ray Diffraction, hardness and optical microscopy

X-ray powder diffraction (XRD) is a rapid analytical technique used for phase identification of materials. The phase analysis of HEAs was done by X-Ray Diffraction (XRD) 30° to 90° using Cu-Kα radiation. The peaks obtained from XRD plot of powders were fitted through High Score Plus (Version3.0d) using pseudo-Voigt function. After peak fitting of all XRD peaks, peak position and then later lattice parameter was calculated. The hardness of all the HEAs was estimated using Vickers hardness tester. The optical micrographs were taken for all the samples using optical microscope.

3.2 Electrochemical analysis

The corrosion behaviour of alloys was investigated using a Potentiostat in 3.5 wt% NaCl solution. The corrosion behaviour of materials was studied using a three-electrode cell with reference (SCE), counter, and working electrodes (HEAs). The icorr and Ecorr values were found out by fitting the curves. These values were found by fitting the polarization curves. Then, the corrosion rate is determined by the formula [10]:

$$CR = \frac{K \bullet EW \bullet I_{corr}}{d \bullet A}$$

where I_{corr} is the corrosion current in amperes and calculated using the Tafel extrapolation method where the cathodic reaction is diffusion controlled, K is a constant equal to 3.27 ×103; EW is equivalent weight.

4. RESULTS AND DISCUSSION

4.1 X-Ray Diffraction of High Entropy Alloys

Figure 1 shows the XRD pattern for HEA1, indicating the formation of majority significant peaks of FCC phase. Similarly, HEA2 showed mainly single FCC phase as shown in Figure 2. The XRD plots for HEA3 (Figure 3) and HEA4 (Figure 4) are almost similar. The significant FCC peaks are (111), (200), and (220).

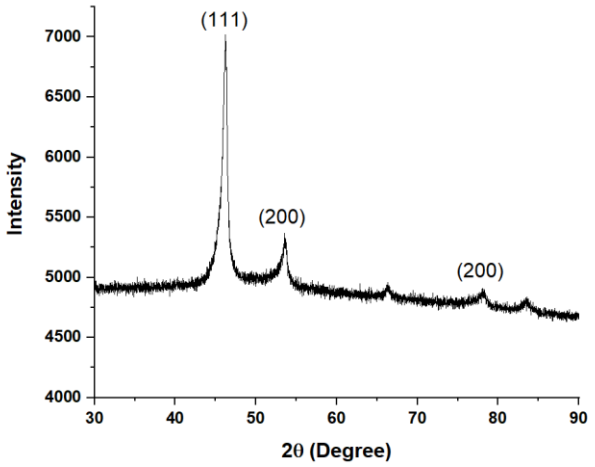

Figure 1 XRD pattern of HEA1

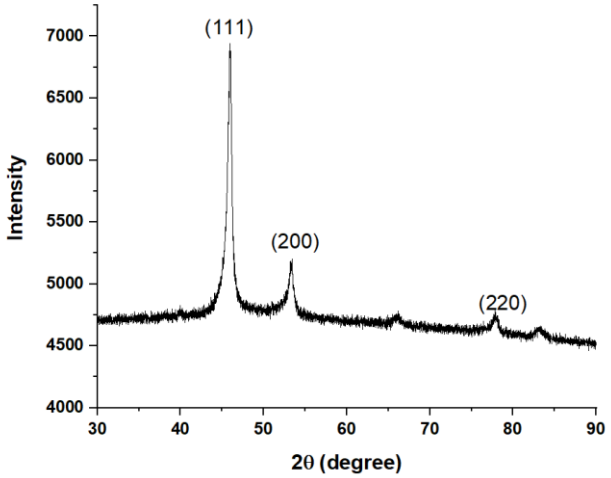

Figure 2 XRD Plot of HEA2

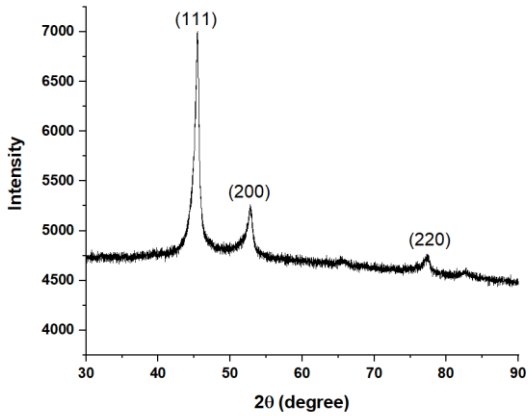

Figure 3 XRD Plot of HEA3.

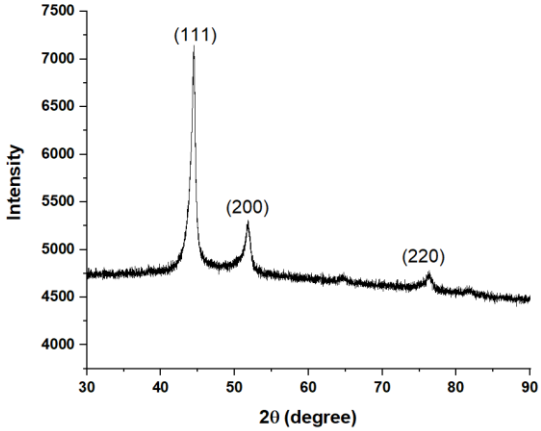

Figure 4 XRD Plot of HEA4.

Figure 5 shows the leftward shift of the most prominent XRD peak from HEA1 to HEA4. It indicates that the lattice parameter is increasing due to large atomic radius of Ti. This extension of lattice parameter can be clearly seen in Table 2.

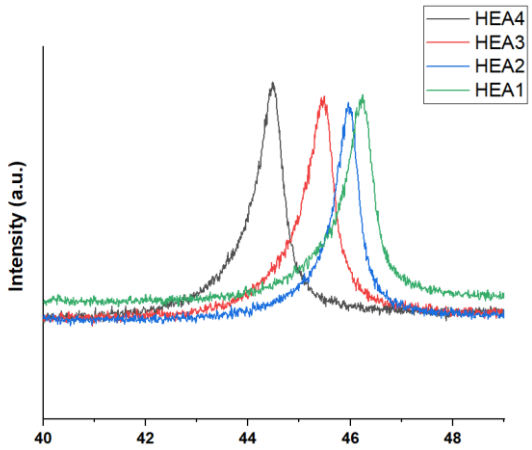

Figure 5 XRD peak shift of HEAs

Table 2 Lattice parameter of HEAs

HEA	Lattice parameter (A)
HEA1	3.559
HEA2	3.567
HEA3	3.582
HEA4	3.587

4.2 Hardness and optical micrographs of HEAs

Figure 6 and Table 3 reveal the hardness of all HEAs. The percentage of Ti in alloy enhanced its hardness due to its large atomic size and impact of solid solution strengthening. As a consequence, Ti acts as a solid solution strengthener, increasing the hardness and strength of alloys. Similar contribution of Ti to hardness has been observed in literature [15], in which the Ti addition to CoCrFeNiAl0.5 increased the hardness value.

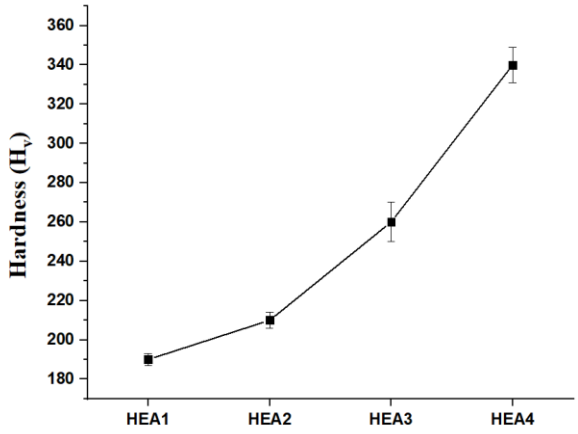

Figure 6 Hardness of the HEAs

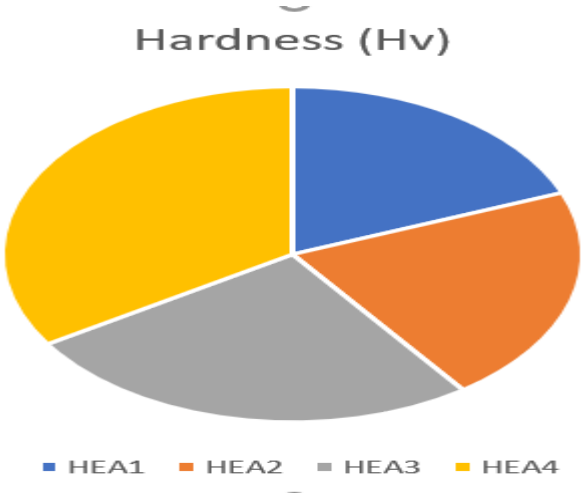

Figure 7 Hardness of HEAs

The optical micrographs were taken of the annealed HEAs as shown in Figure 8. The grains got refined with the increase of Ti content in HEAs because Ti might have hindered the grain growth due to high melting point and precipitations at grain boundaries.

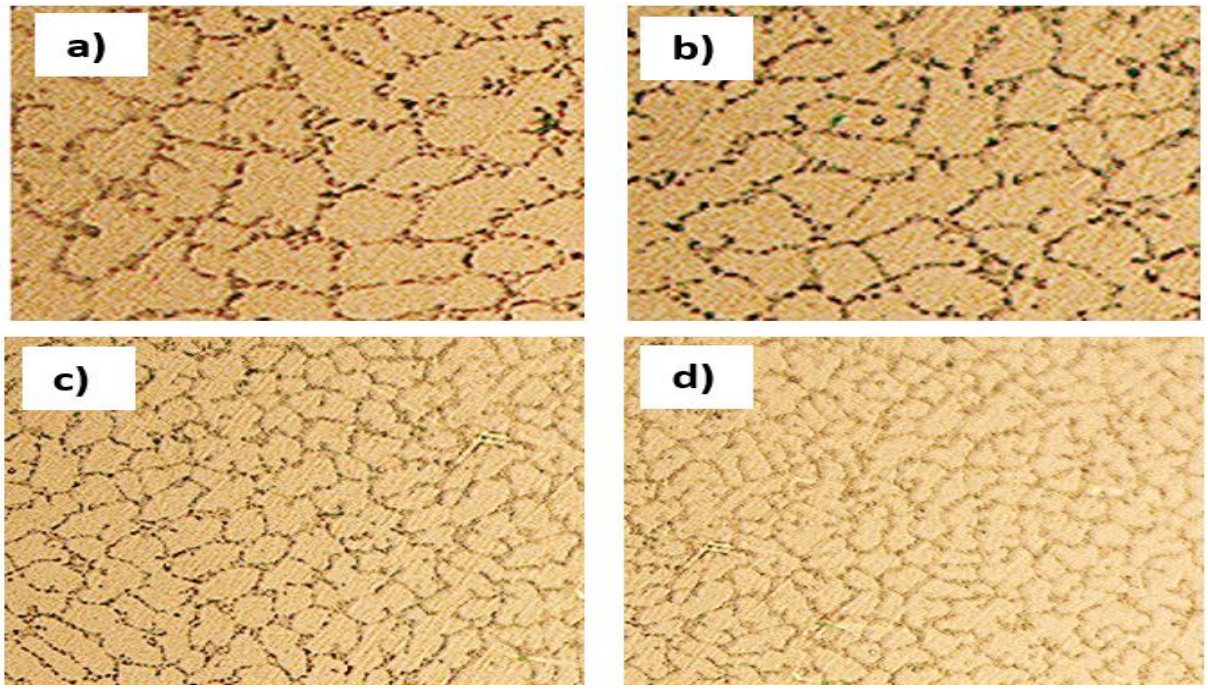

Figure 8 Optical micrographs of a) HEA1, b) HEA2, c) HEA3, and d) HEA4

4.3. Potentiodynamic polarization curves of HEAs in 3.5 wt. % NaCl solution

Figure 9, Figure 10 and Figure 11 reveal that the corrosion potential (Ecorr) increased and icorr decreased with the increase of Ti content, indicating the positive effect of Ti in controlling the corrosion rate. The increased Ecorr shows the decreased tendency to corrosion. The icorr is a kinematic factor, and the decrease of icorr value means the decreased the corrosion rate. For HEA1, the icorr and Ecorr were 2 605.815 µA/cm2 and -452.306 mV, respectively. When increase of Ti in HEA2, Ecorr increased from -452.306 to -406.231 mV and icorr decreased to 1194.371 µA/cm2. With further increase of Ti in HEA4, the corrosion performance became superior as the Ecorr value increased and icorr value decreased continuously as compared to HEA3. The increase in the quantity of Ti lead to decrease in the value of current density (icorr) indicates that the alloy sample with high Ti content formed more corrosion resistant film on the surface in 3.5 wt. % NaCl aqueous solution that hindered the passage any ion or electron through itself which led to decrease in current density.

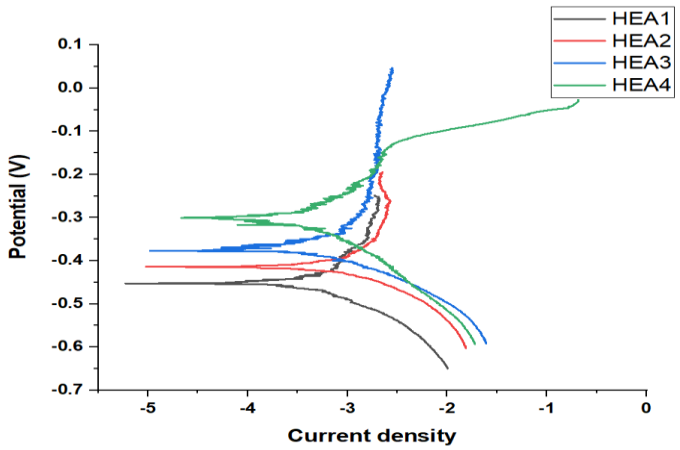

Figure 9 Potentiodynamic polarization curves of HEAs in 3.5 wt. % NaCl solution.

Figure 10 Corrosion potential of HEAs in 3.5 wt. % NaCl solution

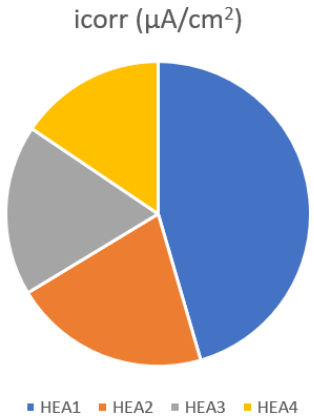

Figure 11 Corrosion current density of HEAs in 3.5 wt. % NaCl solution

Table 3 Corrosion rate of HEAs

Alloy	Corrosion rate (mmpy)
HEA1	24.63
HEA2	11.29
HEA3	9.80
HEA4	8.42

The effect of Ti, seen in the present study, can be compared with the previous studies conducted in literature [16, 17]. However, the obtained corrosion parameter values cannot be directly compared because of different environments and different synthesis techniques. For example, Qui et al. [12] revealed that the Ti-containing Ti0.3(CoCrFeNi)0.7 HEA showed higher Ecorr (-273 mV) and lesser icorr (0.036 µA/cm2) comparing with Ti-free CoCrFeNi alloy (Ecorr=-304 mV, icorr=0.610 µA/cm2). It shows the positive effect of Ti similar to the present study.

5. Conclusion

All the HEAs were synthesized successfully using melting and casting technique. All the samples formed single FCC phase with significant peaks of (111), (200), and (220).The hardness of HEAs increased from HEA1 to HEA4 due to large Ti atomic size. The corrosion resistance in 3.5 wt. % NaCl solution enhanced from HEA1 to HEA4 due to increase of Ti content which helped in passivating the surface effectively and easily.

Conflict of Interest: Authors declare no conflict of Interest

REFERENCES

1. B. R. Anne, S. Shaik, M. Tanaka, and A. Basu, “A crucial review on recent updates of oxidation behavior in high entropy alloys,” SN Appl. Sci., vol. 3, no. 3, pp. 1–23, 2021, doi: 10.1007/s42452-021-04374-1.
2. B. Cantor, I. T. H. Chang, P. Knight, and A. J. B. Vincent, “Microstructural development in equiatomic multicomponent alloys,” Mater. Sci. Eng. A, vol. 375–377, pp. 213–218, 2004, doi: 10.1016/j.msea.2003.10.257.
3. J. W. Yeh et al., “Nanostructured high-entropy alloys with multiple principal elements: Novel alloy design concepts and outcomes,” Adv. Eng. Mater., vol. 6, no. 5, pp. 299–303, 2004, doi: 10.1002/adem.200300567
4. M.J. Yao, K.G. Pradeep, C.C. Tasan, D. Raabe, A novel, single phase, nonequiatomic FeMnNiCoCr high-entropy alloy with exceptional phase stability and tensile ductility, Scr. Mater. 72-73 (2014) 5–8.

5. Z. Li, K.G. Pradeep, Y. Deng, D. Raabe, C.C. Tasan, Metastable high-entropy dual phase alloys overcome the strength-ductility trade-off, Nature 534 (2016) 227–230.
6. T.A. Listyawan, H. Lee, N. Park, A new guide for improving mechanical properties of non-equiatomic FeCoCrMnNi medium- and high-entropy alloys with ultrasonic nanocrystal surface modification process, J. Mater. Sci. Technol. 59 (2020) 37–43.
7. J. Su, D. Raabe, Z. Li, Hierarchical microstructure design to tune the mechanical behavior of an interstitial TRIP-TWIP high-entropy alloy, Acta Mater. 163 (2019) 40–54.
8. C. Dai, H. Luo, J. Li, C. Du, Z. Liu, J. Yao, X-ray photoelectron spectroscopy and electrochemical investigation of the passive behavior of high-entropy FeCoCrNiMox alloys in sulfuric acid, Appl. Surf. Sci. 499 (2020) 143903.
9. Y.Y. Chen, T. Duval, U.D. Hung, J.W. Yeh, H.C. Shih, Microstructure and electrochemical properties of high entropy alloys—a comparison with type-304 stainless steel, Corros. Sci. 47 (2005) 2257–2279.
10. C.C. Yen, H.N. Lu, M.H. Tsai, B.W. Wu, Y.C. Lo, C.C. Wang, S.Y. Chang, S.K. Yen, Corrosion mechanism of annealed equiatomic AlCoCrFeNi tri-phase high-entropy alloy in 0.5 M H2SO4 aerated aqueous solution, Corros. Sci. 157 (2019) 462–471.
11. C. Dai, T. Zhao, C. Du, Z. Liu, D. Zhang, Effect of molybdenum content on the microstructure and corrosion behavior of FeCoCrNiMox high-entropy alloys, J. Mater. Sci. Technol. 46 (2020) 64–73.
12. Y.J. Hsu, W.C. Chiang, J.K. Wu, Corrosion behavior of FeCoNiCrCux high-entropy alloys in 3.5% sodium chloride solution, Mater. Chem. Phys. 92 (2005) 112–117.
13. Y.Z. Shi, B. Yang, X. Xie, J. Brechtl, K.A. Dahmen, P.K. Liaw, Corrosion of AlxCoCrFeNi high-entropy alloys: Al-content and potential scan-rate dependent pitting behavior, Corros. Sci. 119 (2017) 33–45.
14. K.H. Lo, C.H. Shek, J.K.L. Lai, Recent developments in stainless steels, Mat. Sci. Eng. R 65 (2009) 39–104.
15. A. Erdogan, K.M. Döleker, S. Zeytin, Effect of laser re-melting on electric current assistive sintered CoCrFeNiAlxTiy high entropy alloys: Formation, micro-hardness and wear behaviors, Surf. Coatings Technol. 399 (2020) 126179. https://doi.org/10.1016/j.surfcoat.2020.126179
16. Y. Qiu, M.A. Gibson, H.L. Fraser, N. Birbilis, M.A. Gibson, H.L. Fraser, N.B. Corrosion, Y. Qiu, M.A. Gibson, H.L. Fraser, N. Birbilis, Corrosion characteristics of high entropy alloys, Mater. Sci. Technol. Vol. 31, pp. 1235-1243, 2016. https://doi.org/10.1179/1743284715Y.0000000026.
17. R.K. Mishra, P.P. Sahay, R.R. Shahi, Alloying, magnetic and corrosion behavior of AlCrFeMnNiTi high entropy alloy, J. Mater. Sci. vol. 54, pp. 4433–4443, 2019. https://doi.org/10.1007/s10853-018-3153-z.